

Properties of flexible polyurethane foams containing  
isocyanate functionalized kraft lignin  
(<http://dx.doi.org/10.1016/j.indcrop.2017.02.005>)

*Sandra Gómez-Fernández, Lorena Ugarte, Tamara Calvo-Correas, Cristina Peña-Rodríguez, M. Angeles Corcuera, Arantxa Eceiza\**

Group 'Materials + Technologies', Department of Chemical and Environmental Engineering, Faculty of Engineering of Gipuzkoa, University of the Basque Country (UPV/EHU), Plaza Europa 1, Donostia-San Sebastián 20018, Spain

## ABSTRACT

A commercial kraft lignin (k-lignin) was successfully functionalized by means of the reaction of an isocyanate group from isophorone diisocyanate (IPDI) with hydroxyl groups present in lignin (k-IPDI), for their further incorporation in a flexible polyurethane foam (PUF) formulation. The functionalization was confirmed by FTIR and  $^{13}\text{C}$  NMR, as well as by the OH number determination. It was observed that approximately half of the hydroxyl groups present in k-lignin were functionalized. Afterwards, two series of PUF containing 3, 5 and 10% of k-lignin and k-IPDI were prepared by one-shot free rise polymerization. It was observed that the presence of unmodified lignin decreased the reactivity of the system, yielding to longer foaming stages that required the addition of more catalyst to the system. Apart from that, more rigid foams were obtained with k-lignin than with k-IPDI, as it was observed by DSC and compression force deflection (CFD), which values reflected that the presence of k-IPDI contributed to the formation of more flexible foams. It was also found that the functionalization of lignin contributed to a higher chemical attachment of the lignin to the polyurethane matrix as it was observed by lignin extraction experiments. This chemical attachment was reflected on the stress-strain curves which showed that k-lignin containing foams had higher elastic modulus and higher ability to absorb energy than k-IPDI containing ones, which resulted to be more soft and flexible.

## 1. Introduction

Wood is mainly composed by cellulose, hemicelluloses and lignin, apart from extractives and other inorganic compounds. Lignin acts as a binder of the cellulose fibers in the cell walls of vascular plants, providing structural stability as well as performing a protective function as an antimicrobial agent (Barakat et al., 2010). Its aromatic and heterogeneous structure gives place to an amorphous macromolecule that is considered the second most abundant biopolymer on earth only after cellulose, being the main source of aromatic compounds.

Lignin structure is composed by the bonding of three main monomers (Fig. 1). These monomers are known as monolignols and consist on phenylpropane units with different substitutions (p-hydroxyphenil (H), guaiacyl (G) and syringyl (S) units) derived from coumaryl, coniferyl and

sinapyl alcohol, respectively (Gosselink et al., 2004a). The prevalence of one unit or another will depend on the vegetable species of origin; for instance, G units are predominant in softwood lignin, a mixture G and S units in hardwood and finally H units are more abundant in lignin derived from annual plants.

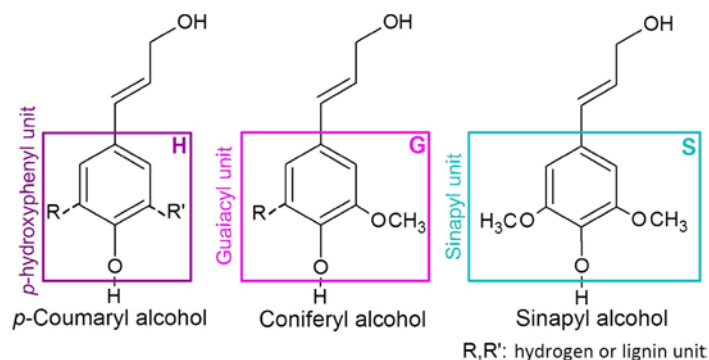


**Fig. 1.** Main structural units that compose lignin structure

These monomers are connected by different C-C and ether linkages, such as  $\beta$ - $\beta$ ,  $\beta$ -1, 4-O-5 and  $\beta$ -O-4, being the latter the most common, especially in softwood lignin (Laurichesse and Av erous, 2014; Li et al., 1997). These linkages hamper the isolation of lignin without its fractionation. Nowadays different processes are used for the extraction of lignin, such as enzymatic acidolysis, ionic liquid pretreatment, organosolv, kraft and liginosulfonate processes, being the last two the most used and developed at industrial scale (Li et al., 2015).

The kraft pulping method is used for the conversion of wood (both softwood and hardwood) into pulp for the further production of paper. In this process, the wood is cooked in digesters where a great part of the lignin contained in wood is degraded into different molecular weight fragments. These fragments are dissolved in an aqueous solution of sodium hydroxide and sodium sulfide together with carbohydrates obtained from hemicelluloses and inorganic salts, forming the so called black liquor. An appropriate treatment and purification of this black liquor gives rise to the isolation of kraft lignin.

The integration of wood-related industrial processes with biorefineries, would provide added value to byproducts such as lignin, and would provide a great source of renewable materials and energy. Nevertheless, the heterogeneous composition makes difficult to obtain large lignin batches with a homogeneous quality for chemical and materials production. For this reason, softwood kraft lignin, which is characterized for being more reactive and for having a more homogeneous structure than hardwood lignin (Gellerstedt, 2015), is the perfect candidate for large scale production.

Even though most of this lignin is commonly burned as internal production of energy for the pulping process, nowadays more and more quantities are commercialized for its use as additive, dispersant or dye (Holladay et al., 2007). Research is nowadays focused on taking advantage of lignin in high value-added applications such as the obtaining of fine chemicals (Bouxin et al., 2015; Fan et al., 2015), carbon fiber production (Kadla et al., 2002; Mainka et al., 2015) and materials containing lignin not only as an additive (Morandim- Giannetti et al., 2012), but also as a part of the formulation (Zhang et al., 2013).

The use of lignin in polyurethane chemistry is promising since lignin provides the hydroxyl groups needed for urethane linkage formation. In this way, several approaches have been developed in order to obtain polyurethanes containing lignin not only as an additive (Ciobanu et al., 2004), but also as a replacement of the main reactive materials using oxypropylated or liquefied lignin as a promising environmental friendly alternative of polyols derived from fossil sources (Cateto et al., 2009; Cinelli et al., 2013).

Flexible polyurethane foams (PUF) constitute a large market of the polyurethane family. PUF are a commodity material used in several applications such as automotive seating, upholstery, mattresses, packaging and other similar everyday applications. They are obtained by the reaction of three main reactants: a polyol (with functionality higher than 2), a diisocyanate and a blowing agent (usually water). Other additives such as surfactants and catalysts are also used in order to balance the reactions involved in the foaming process. They represent a very versatile group of polymers owing to the possibility to tailor their properties depending on the nature and characteristics of the used reactants (Ashida, 2006). Nonetheless, these reactants dependence on fossil resources and the increasing awareness of environmental issues such as climatic change, greenhouse emissions, petroleum depletion and so on, have focused the efforts of diverse scientific fields into the replacement of fossil sources by renewable ones in order to obtain chemicals such as polyols derived from vegetable oils (Calvo- Correias et al., 2015), or the use of very diverse industrial wastes or byproducts, such as coffee (Soares et al., 2015) or lignin, as additives or as part of the reactant mixture for obtaining eco-friendly foams.

Nevertheless, the addition of lignin as a reactive filler in free-rise flexible polyurethane foams can be difficult in regard to the rapid foaming process that requests highly reactive compounds in order to have a conversion high enough to support the rapidly formed porous structure. The presence of lignin hampers the polymerization due to its complex structure and the low reactivity of its hydroxyl groups as a consequence of steric hindrance (Tejado et al., 2008). This problem could be overcome through the replacement of these hydroxyls for more reactive groups such as isocyanate. Notwithstanding, little attention has been paid to the use of lignin as replacement of the isocyanate counterpart, although some works can be found where different prepolymers are prepared by the functionalization of lignin with this group (Chauhan et al., 2014; Rozman et al., 2001).

For this reason, in this work the functionalization of a commercial kraft lignin (k-lignin) with a highly reactive group such as isocyanate, has been carried out successfully reacting part of the hydroxyl groups present in lignin with isophorone diisocyanate (IPDI), thus forming urethane bonds between them and leaving also free isocyanate groups for their further reaction with the other components of the polyurethane matrix during the foaming process. The characterization of k-lignin and the isocyanate functionalized lignin (k-IPDI) was carried out by means of elemental analysis, Fourier transform infrared spectroscopy (FTIR), <sup>13</sup>C nuclear magnetic resonance (<sup>13</sup>C NMR) in both solid and liquid state, scanning electron microscopy (SEM), differential scanning calorimetry (DSC), and thermogravimetric analysis (TGA).

In order to compare the impact of lignin functionalization, a reference foam (without lignin) and

a series of foams containing the same amount of lignin (3, 5 and 10 wt.%) from k-lignin and k-IPDI were prepared. Their properties were analyzed by means of FTIR, optical microscopy, SEM, DSC, TGA and compressive mechanical properties.

## 2. Experimental procedure

### 2.1. Materials

Southern pine kraft lignin, k-lignin (Domtar's BioChoice™) was kindly provided by UPM Biochemicals (Finland). The acetylation of k-lignin was performed for its further characterization by GPC and <sup>13</sup>C NMR, using acetic anhydride (98%, Panreac) and pyridine (99%, Panreac). Ethanol (>99.8%, Panreac), HPLC grade chloroform (>99.8%, Lab-Scan Analytical Sciences) and diethyl ether (99.7%, Panreac) were used in the process of washing the derivatized lignin (ac-lignin).

The functionalization of k-lignin with isocyanate groups was carried out using isophorone diisocyanate, IPDI (>99.5%, Desmodur® I, Covestro), with a NCO content of 37.8%. HPLC grade tetrahydrofuran, THF (>99.8%, Macron Fine Chemicals) was used as reaction medium and dibutyltin dilaurate, DBTDL (>95%, Sigma Aldrich) as selective catalyst for the reaction of hydroxyl groups from lignin with the secondary NCO groups of IPDI (Ono et al., 1985). HPLC grade toluene (>99.8%, Lab-Scan Analytical Sciences) was used to wash the functionalized lignin.

Flexible polyurethane foams were prepared using two sides of formulation (A and B). The side B was composed by the blend of a castor oil derived polyether polyol from BASF, Lupranol Balance®50 (LB50, OH-number = 50 mg KOH g<sup>-1</sup>, functionality = 2.7 and viscosity = 837 mPa s at 25 °C), deionised water as blowing agent and additives (all from Evonik) for balancing the blowing and gel reactions during the foaming process. Stannous octoate was used as organometallic co-catalyst (Kosmos® 29) for the balance of the gelling reaction, whereas the amine catalyst Tegoamin® B 75 was employed for balancing both blowing and gelling reactions. A silicone surfactant (Tegostab® B 4900) was used for stabilizing the B-side mixture and the structure of the foam. The side A was constituted by the mixture of 2,4- and 2,6- toluene diisocyanate (TDI) isomers in a 80:20 ratio (≥99.5%, Desmodur® T-80, Covestro) containing a 48.2% NCO, and was used without further purification.

### 2.2. Lignin acetylation

The acetylation of lignin was performed following a method proposed elsewhere (Lundquist, 1992) in order to determine its molecular weight by Gel Permeation Chromatography (GPC) and also to quantify the hydroxyl content by quantitative <sup>13</sup>C Nuclear Magnetic Resonance (NMR). Briefly, 20 mg of k-lignin were dissolved in a 1:1 (v/v) acetic anhydride-pyridine mixture and kept stirring 24 h at room temperature. The washing process was conducted as follows: absolute ethanol was added to the mixture, stirred during 30 min and then removed with a rotary evaporator, repeating this step for seven cycles using the ethanol to drag the pyridine and the acetic acid from the sample. Thereafter the ac-lignin was dissolved in chloroform and added dropwise to diethyl ether, washed three times by centrifugation and dried under vacuum at 50 °C for 24 h.

### 2.3. Preparation of IPDI modified lignin

Kraft lignin was grounded in a mortar and dried at 50 °C for 24 h prior to its functionalization with IPDI. Once dried, k-lignin (20 g) was dissolved in 100 mL of THF using a magnetic stirrer. Afterwards IPDI was weighed into a round bottom flask in a 3/1 NCO/OH molar ratio and heated up to 60 °C under nitrogen atmosphere. Then, DBTDL (0.1% of the total weight) was added to the IPDI and stirred (at 600 rpm) during few minutes, followed by the addition of the lignin solution to the flask using a dropping funnel while kept at 60 °C for 24 h. Thereafter, the formed solid was separated maintaining the vigorous stirring in the flask. The reaction was by centrifugation, washed with toluene and centrifuged repeatedly (at least three times) at 4500 rpm during 5 min, replacing the used toluene for fresh one after each centrifugation in order to remove vacuum oven at 75 °C for 24 h and then the vacuum was kept at the remaining unreacted IPDI. Finally, the slurry was dried in a room temperature for the following 48 h. The obtained k-IPDI was grounded and sieved in order to obtain a homogeneous particle size.

### 2.4. Preparation of flexible polyurethane foams

Two series of flexible polyurethane foams containing the same amount of lignin regardless the isocyanate content of the k-IPDI (which was taken into account to maintain the OH-NCO ratio) were produced, in addition to a reference foam without lignin (PUF-REF). The lignin content of the foams was set at 3, 5 and 10% (by weight) for both k-lignin (PUF-3%kl, PUF-5%kl and PUF-10%kl) and k-IPDI containing foams (PUF-3%kIPDI, PUF-5%kIPDI, PUF-10%kIPDI). PUF with k-lignin were prepared dissolving previously dried lignin in 50 mL. Then, the k-lignin solution was added slowly to the polyol and stirred vigorously during 1 h at room temperature. The THF was then removed using a rotary evaporator until constant mass was achieved. The k-lignin precipitated during THF removal, forming a stable and fine dispersion of the solids in the polyol. Once the k-lignin/LB50 mixture was prepared, the polyurethane foams were manufactured according to the procedure reported previously (Gómez-Fernández et al., 2016) by one shot open mold polymerization, plus a postcuring process at 150 °C during 24 h. After this thermal treatment, the disappearance of free NCO was confirmed by FTIR in different regions of the foams. In case of k-IPDI containing PUF, the functionalized lignin was introduced directly into the polyol and homogenized by rotor-stator mixing at 12,000 rpm during few minutes. All the foams were formulated with the same amount of blowing agent, surfactant and an excess of 10% of isocyanate (corresponding to an isocyanate index of 110) without taking into account the OH content of the lignin in the formulation owing to its low reactivity. Nevertheless, the catalyst formulation had to be increased in case of k-lignin containing samples, since the presence of lignin affected the reactivity of the polymerization process hampering the formation of acceptable foams. Thus, amine and organometallic catalyst were adjusted (increasing their amount in 0.5 and 0.6 parts per hundred of polyol with respect to PUF-REF and k-IPDI containing foams) in order to yield the gelling time quickly enough to avoid the collapse of the foam (Szycher, 2013). Thermal, morphological and mechanical characterization of the foams was performed to postcured samples.

## 2.5. Measurements and characterization

### 2.5.1. Lignin determination and characterization

The moisture content of the raw lignin was analyzed by TGA (TGA/SDTA 851, Mettler Toledo) in nitrogen atmosphere heating the sample from 25 to 200 °C at a heating rate of 10 °C min<sup>-1</sup>. This value was confirmed gravimetrically drying the lignin in an oven at 50 °C for 24 h, so as to determine whether this temperature was enough to get a dried lignin in 24 h. Since the obtained values were similar, the average value of both was reported.

Acid insoluble lignin (AIL) was determined following TAPPI T249 cm-85 and TAPPI T222 om-83 methods. Briefly, 3.75 mL of ice-cooled 12 M sulfuric acid (H<sub>2</sub>SO<sub>4</sub>) were added to 0.375 g of dried lignin (Gosselink et al., 2004a) and kept at 30 °C during 1 h. Demineralised water was then added and the mixture was kept boiling at 100 °C for 3 h. The suspension was cooled, filtered with a G4 glass filter and washed with hot water. The resulting solid was weighed after being dried at 105 °C and the filtrate was kept for measuring the acid soluble lignin (ASL) content.

ASL was determined by UV–vis spectroscopy (Dence, 1992), placing a sample of the clear filtrate from the previous step in a silica absorption cell with a 10 mm light path. The absorbance was measured at 205 nm using a 3% H<sub>2</sub>SO<sub>4</sub> solution as a blank and the sample was diluted with the H<sub>2</sub>SO<sub>4</sub> solution until obtaining absorbance values ranging between 0.2 and 0.7. Beer's Law was used in order to calculate the acid soluble lignin content (Eq. (1)), where  $b = 1$  cm;  $a = 110$  L g<sup>-1</sup> cm<sup>-1</sup>,  $V_D$  is the volume of the diluted sample and  $V_O$  the volume of the original sample.

$$\text{Acid soluble lignin content, } gL^{-1} = \frac{\text{Absorbance } (A)}{b \text{ (light path, cm)} \cdot a \text{ (absorptivity, } Lg^{-1}cm^{-1})} \cdot \frac{V_D}{V_O} \quad (1)$$

The ash content of the kraft lignin was determined following the ASTM E1755-01 standard. Firstly, the lignin was oven-dried at 105 °C during 24 h. Two samples of approximately 1 g were treated in a muffle furnace at 525 °C during 5 h and the weight of the remaining residue was recorded as the ash content, given relative to the weight of dried lignin. This ash was thereafter used to calculate the acid insoluble ash (AI ash) content for correcting the AIL value following the TAPPI T245 om-94 standard, adding firstly 20 mL of 65% (w/w) nitric acid to the ash, heating it up and keeping it boiling until having a residual volume of around 10 mL. Then, 4 mL of 96% (w/w) sulfuric acid were added and heated again until white fumes were evolved. The mixture was cooled down to room temperature and finally 50 mL of demineralised water were added and boiled for 5 min. After filtrating, washing and drying, the remaining solid was weighed for correcting the acid insoluble lignin content.

The presence of sugar impurities was determined by High Performance Liquid Chromatography using a Jasco LC Net II/ADC with a ROA Organic Acid column from Phenomenex, equipped with a refractive index detector and a photodiode array detector. 0.005 NH<sub>2</sub>SO<sub>4</sub> was used as mobile phase, performing the assay with a flow rate of 0.35 mL min<sup>-1</sup> at 40 °C. High purity standards of d-(+)-glucose, d-(+)-xylose, and d-(-)-arabinose (Fluka) were used for calibration (Gordobil et al., 2014). The analysis was performed twice. The approximate hydroxyl number of both k-lignin and k-IPDI were determined following the ISO 14900:2001(E) standard for polyols with steric

hindrance carrying out the acetylation of the sample with a mixture of acetic anhydride and pyridine using imidazole as catalyst. After the acetylation, a back titration was performed with 0.5 N NaOH. The hydroxyl number was also confirmed by quantitative  $^{13}\text{C}$  NMR.

#### 2.5.2. *Chemical analysis*

The carbon, hydrogen, nitrogen and sulfur content of k-lignin and k-IPDI lignin was determined by elemental analysis using aEurovector EA 3000 atomic absorption spectrometer heated at 980 °C with a constant flow of helium. The content of sodium was analyzed by inductively coupled plasma optical emission spectrometry (ICP-OES) in a Mettler Toledo Optima 8300 equipment, solving the lignin samples in concentrated nitric acid and subsequently diluting them with deionized water to 15 mL.

#### 2.5.3. *Average molecular weight*

Number and weight average molecular weight values ( $\overline{M}_n$  and  $\overline{M}_w$ ) and polydispersity (PD) of the derivatized k-lignin was determined by GPC using a Thermo Scientific UltiMate 3000 equipped with four Phenogel GPC columns from Phenomenex (particle size of 5  $\mu\text{m}$  and porosity of 105, 103, 100 and 50 Å) and a RefractoMax521 refractive index detector. The analysis was carried out at 30 °C with a flow rate of 1 mL min $^{-1}$  with THF as the mobile phase and an injection volume of 50  $\mu\text{L}$ . The samples were prepared dissolving 1% by weight of ac-lignin in THF and filtering them with 0.20  $\mu\text{m}$  pore sized nylon filters. The  $\overline{M}_w$  values were referred to monodisperse polystyrene standards.

#### 2.5.4. *Structural characterization*

The analysis of the functional groups of k-lignin and the successful functionalization with NCO of k-IPDI was determined by FTIR (Nicolet-Nexus) using KBr pellets and performing the assay between 4000 and 400 cm $^{-1}$  at room temperature, performing 64 scans with 4 cm $^{-1}$  resolution. Both k-lignin and k-IPDI were dried at 50 °C during 24 h prior to the pellet preparation. The influence of the lignin on the reactivity of the foam was also analyzed by FTIR, carrying out the assay 24 h after the polymerization but before the postcuring process, using a Specac attenuated total reflectance accessory (Golden Gate<sup>®</sup>ATR device) in the range between 4000 and 600 cm $^{-1}$ , performing 32 scans with a resolution of 4 cm $^{-1}$ . The determination of functional group content in k-lignin, such as methoxyl, carbonyl and hydroxyl groups, was performed by  $^{13}\text{C}$ NMR. Quantitative  $^{13}\text{C}$  NMR was performed in k-lignin and ac-lignin samples aiming to determine the primary, secondary and phenolic hydroxyl (OH(I), OH(II) and OH( $\phi$ ), respectively) group content present in unmodified lignin. For this purpose, dried k-lignin and ac-lignin samples were solved in DMSO- $d_6$  (10 mg of solid in 1 mL of solvent). The signals present in ac-lignin at 170.6, 169.9 and 169.1 ppm (corresponding to OH(I), OH(II) and OH( $\phi$ ), respectively) were integrated with respect to the aromatic region of lignin assuming the presence of six carbons between 100 and 160 ppm. The total hydroxyl group content obtained by this technique was compared to the results obtained by using the aforementioned ISO 14900:2001(E) standard.

The liquid  $^{13}\text{C}$  NMR spectra were registered on a Bruker Avance 500 spectrometer, equipped

with a BBO probe with gradient in Z axis. A decoupled sequence zgdc from Bruker library was used at 125.77 MHz. A time domain of 64 k, and a spectral width of 31000 Hz were used. The interpulse delay was set to 2 s and the acquisition time to 1.5 s. For each spectrum 32000 scans were accumulated.

Additionally, k-IPDI was qualitatively characterized by solidstate  $^{13}\text{C}$ -cross-polarization magic angle spinning (CP/MAS) NMR, performing directly the assay over dried k-lignin and k-IPDI. The spectra were recorded on a Bruker 400 AVANCE III WB spectrometer 9.40T, using a 4 mm DVT-MAS probe at a spinning rate of 10 kHz. The standard cross-polarization pulse sequence (100.6 MHz), a time domain of 2 k, a spectral width of 29 kHz, a contact time of 1.5 ms and an interpulse delay of 5 s were used.

#### 2.5.5. *Morphology*

The morphology of the particles and the cellular structure of the polyurethane foams were characterized by SEM using a JEOLJSM-7000F equipment operating at 10 kV and a surrounding beam current of 10 pA, taking secondary electron images. Dried samples were placed over a double-sided carbon-based conductive tape and covered with a 10 nm chromium layer. Both k-lignin and k-IPDI powders were milled before drying. The open cell content of the foams was measured by using a porosity tester (MicroFlo, IES). The test was carried out at 20 °C measuring the air passing through the cellular structure of the foam, parallel to grow direction. Four specimens were tested for each sample, and the average open cell content was reported.

#### 2.5.6. *Thermal properties*

The glass transition temperature of the raw lignin and the isocyanate-modified lignin was analyzed using a Mettler Toledo DSC822 equipment. Around 5 mg of previously dried lignin (24 h at 50 °C) were used and two scans were performed in order to remove the thermal history of the samples, from -60 to 200 °C at a heating rate of 10 °C min<sup>-1</sup>, with a nitrogen flow of 10 mL min<sup>-1</sup>. In case of polyurethane foams, the DSC analyses were conducted in a Mettler Toledo DSC3+ equipment, from -120 to 200 °C at a heating rate of 30 °C min<sup>-1</sup> under a nitrogen flow of 10 mL min<sup>-1</sup>. Two scans were also performed in samples of approximately 5 mg. The thermal degradation of lignin and polyurethane foams was studied using a TGA/SDTA 851 from Mettler Toledo. Approximately 5 mg of sample was analyzed from 25 to 800 °C at a heating rate of 10 °C min<sup>-1</sup>, under a nitrogen flow of 10 mL min<sup>-1</sup>.

#### 2.5.7. *Viscosity, density and cell size*

The viscosity of the k-lignin and k-IPDI dispersions with the polyol was performed prior to foam preparation, recording the values at 25 °C within a shear rate range from 10 to 100 s<sup>-1</sup> using a Thermo Haake Viscotester iQ equipped with P35/Ti parallel plates. The density of the polyurethane foams was measured gravimetrically according to the ASTM D-3574-11 test A standard, using four specimens with dimensions of 50 × 50 × 25 mm<sup>3</sup> for each foam. The average cell size of the pores constituting the foamed structure and the average strut width were calculated using an Eclipse E600 (Nikon) optical microscope, measuring at least 50 cells on

each sample, on the surface perpendicular to the foam growth.

#### 2.5.8. *Lignin extraction from the foam*

Polyurethane foams containing lignin were subjected to extraction with a mixture of 1,4-dioxane/water (90/10, v/v) to determine to what extent was the lignin chemically attached to the polymeric matrix. Briefly, around 0.7 g of foam were cut into cubes of approximately 5 x 5 x 5 mm<sup>3</sup> and were placed inside a cellulose cartridge, performing thereafter the extraction with the dioxane/water mixture using a Soxhlet extraction kit during 24 h. The mass of the foams was weighed before and after the extraction process. The procedure was performed once per sample, as a preliminary study of the chemical attachment of the lignins to the matrix. The mass loss related to polyurethane, which was registered in PUF-REF, was corrected in lignin containing foams in order to consider solely the lignin mass loss.

#### 2.5.9. *Mechanical properties*

The resilience of the foams was calculated following the ASTM D-3574-11 test H standard, using a Qualitest Ball Rebound Tester in the operating mode 3. The average value of 9 measurements for each sample in the foam rise direction was reported. The compression force deflection (CFD) value of the foams, which gives an insight into their firmness, was measured in the foam rise direction according to the ASTM D-3574-11 test C standard, using a MTS equipment with a load cell of 10 kN equipped with compression plates. Two fast pre-compressions were previously performed until a deformation of 75% at a crosshead rate of 250 mm min<sup>-1</sup>. After 5 min of resting without contact with the upper compression plate, the measurement of CFD was conducted at 50 mm min<sup>-1</sup> until 50% of deformation, registering the stress value after 60 s of compression.

The specific elastic modulus, compressive stress at 10% of deformation and the energy storage of the foams were determined from the stress-strain curves using also the MTS equipment with a 10 kN load cell. Four specimens for each foam sample with dimensions of 50 x 50 x 25 mm<sup>3</sup> were tested at a crosshead rate of 5 mm min<sup>-1</sup> until a deformation of 70%. The elastic modulus was calculated as the slope from the initial linear behavior and the energy storage as the area below the stress-strain curves until 50% of strain.

### **3. Results and discussion**

#### 3.1. *Lignin characterization*

##### 3.1.1. *Lignin determination*

The determination of total lignin content was carried out in order to confirm the purity of the k- lignin. The lignin was characterized without further purification than drying in an oven (24 h at 50 °C) owing to its high moisture content (28.43%). Table 1 shows the composition of the k-lignin on a dry basis, reflecting that it was a high purity lignin, reaching nearly a 90% of total lignin content even though having detected a small amount of sodium and sulfur due to its kraft origin (Table 2). Not only was low the sugar impurity content (0.79%), perceiving only the presence of xylose, but also the inorganic impurities (ash content, 1.28%), as it is common in

kraft lignins due to the precipitation method from the black liquor.

**Table 1.** Composition of k-lignin.

	<b>k-lignin</b>
Total lignin content (wt.%)	89.38
<i>AIL</i>	88.27
<i>ASL</i>	1.11
Ash (wt.%)	1.28
Al ash (wt.%)	ND
Sugars (wt.%)	0.79
<i>Arabinose</i>	ND
<i>Glucose</i>	ND
<i>Xylose</i>	0.79
<i>Mannose</i>	ND
$\bar{M}_n$ (g mol <sup>-1</sup> )	3696
$\bar{M}_w$ (g mol <sup>-1</sup> )	7780
PD ( $\bar{M}_w / \bar{M}_n$ )	2.10

ND: Not detected.

**Table 2.** Chemical composition, hydroxyl number and isocyanate content of k-lignin and k-IPDI.

	<b>k-lignin</b>	<b>k-IPDI</b>
Elemental analysis (wt.%)		
<i>C</i>	64.1	63.37
<i>H</i>	5.8	6.81
<i>N</i>	0.25	5.29
<i>O</i>	29.13	21.22
<i>S</i>	1.78	1.84
<i>Na</i>	0.68	0.01
<i>C<sub>9</sub> unit formula</i>	C <sub>9</sub> H <sub>8.28</sub> S <sub>0.10</sub> O <sub>2.58</sub> (OCH <sub>3</sub> ) <sub>0.74</sub>	C <sub>9</sub> H <sub>10.84</sub> S <sub>0.11</sub> O <sub>1.14</sub> (OCH <sub>3</sub> ) <sub>0.77</sub> (NHCO) <sub>0.38</sub> (NCO) <sub>0.38</sub> <sup>a</sup>
<i>C<sub>9</sub> unit Mw (g mol<sup>-1</sup>)</i>	184	193
<i>Total OH content (mmol g<sup>-1</sup>) according to ISO14900:2001(E)</i>	7.33	3.52

a

*C<sub>9</sub> unit formula of k-IPDI was calculated assuming that the same amount of OCH<sub>3</sub> in k-lignin, calculated by <sup>13</sup>C NMR, was present in k-IPDI sample, and that only half of the nitrogen present reacted with the hydroxyl groups from lignin.*

These values are in agreement with those reported in the literature for other industrial kraft lignins (Gosselink et al., 2004b; Passoniet al., 2016). Regarding the average molecular weight determination of the k-lignin by GPC, it was derivatized to ac-lignin in order to get increased solubility in the mobile phase (THF) (Gellerstedt,1992). The average molecular weight resulted to relatively low ( $7780 \text{ g mol}^{-1}$ ), whereas the PD of the sample indicated a narrower weight distribution, as it is usual in commercial industrial lignin (Sarkanen et al., 1984).Regarding the functionalization of the k-lignin sample, it was mandatory to determine the amount of hydroxyl groups in its structure by means of OH number determination. It was observed that the hydroxyl content of the k-lignin was in accordance to those values from other commercial kraft lignins (Cateto et al., 2008). A distinct decrease in the hydroxyl content was registered in k-IPDI as a consequence of the reaction between some of the hydroxyl groups of the lignin with the IPDI, evidencing the different reactivity of the hydroxyls of the lignin depending of their chemical environment. Therefore, the difference between the OH number of k-lignin and k-IPDI showed up that  $3.81 \text{ mmol OH g}^{-1}$  reacted with isocyanate. The conversion of this OH consumption into nitrogen percentage (5.33%) is in accordance with the nitrogen content obtained by elemental analysis in k-IPDI (5.29%).

### 3.1.2. Structural characterization

FTIR allows distinguishing the most relevant units composing the lignin structure. Fig. 2 and Table 3 show the most representative functional group vibrations in the infrared spectrum. The bands appearing at  $1269$ ,  $1146$ ,  $853$  and  $814 \text{ cm}^{-1}$  are the characteristic vibrations of the guaiacyl units (G), common in softwood lignin. The broad band corresponding to O-H stretching vibration at  $3391 \text{ cm}^{-1}$  in k-lignin decreased drastically in ac-lignin corroborating the consumption of hydroxyl groups during its chemical treatment. The broad O-H peak appearing as an average of the hydrogen bonded and free hydroxyl groups in the unmodified lignin, was replaced by two low intensity peaks at around  $3644$  and  $3527 \text{ cm}^{-1}$ , reflecting non-hydrogen bonded aliphatic and phenolic OH groups (Stuart, 2004). Moreover, the appearance of an intense peak at  $1766 \text{ cm}^{-1}$  with a shoulder at  $1740 \text{ cm}^{-1}$  corresponding to aliphatic and aromatic C=O stretching vibration respectively, and a broad band around  $1200 \text{ cm}^{-1}$  related to C-O-C and C-C stretching vibrations in esters, confirmed the successful acetylation of k-lignin.

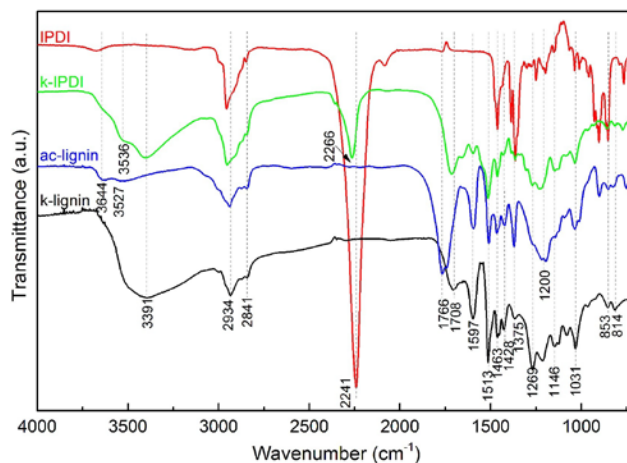


**Fig. 2.** FTIR spectra of k-lignin, ac-lignin, k-IPDI and IPDI.

**Table 3.** k-lignin, ac-lignin and k-IPDI functional groups and their respective FTIR wavenumber.

<b>Functional group</b>	<b>k-lignin Wavenumber (cm<sup>-1</sup>)</b>	<b>ac-lignin Wavenumber (cm<sup>-1</sup>)</b>	<b>k-IPDI Wavenumber (cm<sup>-1</sup>)</b>
Free aliphatic and aromatic O—H str	–	3644, 3527	3644, 3536 <sup>a</sup>
O—H str	3391	–	3391
N—H str	–	–	3391
C—H str in methylene (—CH <sub>2</sub> —)	2934	2934	2951
C—H str in methyl (CH <sub>3</sub> —)	2841	2841	2848
NCO str	–	–	2266
C=O str (aliphatic)	–	1766	–
C=O str (aromatic)	–	1740	–
C=O str of fatty esters, unconjugated ketones, carbonyls and ester groups	1708	–	1712
Urethane C=O str	–	–	–
C—H aromatic ring skeletal vibration and C=O str	1597	1597	1597
C—H aromatic ring skeletal vibration	1513	1513	1513
C—H asymmetrical deformation in —CH <sub>2</sub> — and CH <sub>3</sub> —	1463	1463	1463
Aromatic ring skeletal vibrations, C—H in-plane deformation	1428	1428	1428
Phenyl —OH, aliphatic str in —CH <sub>3</sub>	1375	1375	1375
G ring breathing and C=O str	1269	1269 <sup>a</sup>	1269
C—O—C and C—C str	1211	1200	1224
Aromatic C—H in plane deformation (typical from G units)	1146	1146	1146
Aromatic C—H in plane deformation, —OH deformation in primary alcohols and unconjugated C=O str	1031	1031	1031
C—H out of plane in 2, 5 and 6-positions of G units	853, 814	853, 820	853, 814

a

Shoulder.

In case of k-IPDI, the decrease in the intensity of O-H stretching was not as pronounced as it was in ac-lignin due to the overlap-ping of the signal of sterically hindered unreacted hydroxyl groups and the stretching vibration of the N-H linkage of the urethane group formed during reaction between the lignin and the IPDI. The appearance of an intense peak at 2266  $\text{cm}^{-1}$  denoted the presence of free NCO groups, since the use of DBTDL favored the reaction of the lignin hydroxyl groups with the most reactive NCO group from the IPDI, which is the secondary one, as it was reported before (Onoet al., 1985). The displacement to higher wavenumber and increase of the intensity of C=O stretching at 1712  $\text{cm}^{-1}$ , together with the appearance of a peak at 1660  $\text{cm}^{-1}$  also confirmed the presence of urethane bonds between lignin and IPDI. The functional group content per lignin empirical  $\text{C}_9$  unit formula was estimated by means of NMR spectroscopy (Fig. 3).

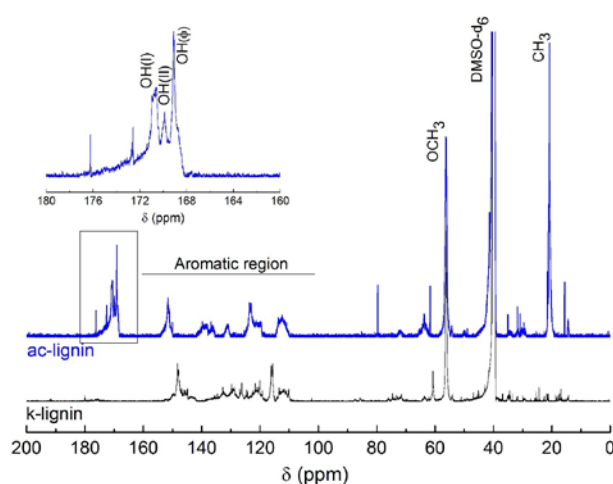


**Fig. 3.**  $^{13}\text{C}$  NMR spectra of unmodified (k-lignin) and acetylated lignin (ac-lignin).

**Table 4.** k-lignin functional group content determination by quantitative  $^{13}\text{C}$  NMR.

	<b>Functional group</b>	<b><math>\delta</math> (ppm)</b>	<b>C atoms per <math>\text{C}_9</math> unit</b>	<b>Amount in lignin (<math>\text{mmol g}^{-1}</math>)</b>
$^{13}\text{C}$ NMR	COOH and CHO	160–200	0.01	0.054
	Total OH	168–178	1.28	6.957
	OH( $\phi$ )	168–169.9	0.46	2.500
	OH(aliphatic)	169.9–172	0.82	4.456
	OH(I)	170.3–172	0.59	3.207
	OH(II)	169.9–170.3	0.23	1.250
	OCH <sub>3</sub>	55.4–58	0.74	4.022

This formula is an approximation calculated to give an idea of the functional groups available in the  $\text{C}_9$  structural unit of lignin. Quantitative  $^{13}\text{C}$  NMR spectroscopy, with a wider spectral width and better resolution than  $^1\text{H}$  NMR, allowed to report the functional groups per aromatic ring

in k-lignin, distinguishing primary, secondary and phenolic hydroxyl groups in acetylated lignin samples (Faix et al., 1994). The value of the integration can be considered as mol% and its conversion to mmol g<sup>-1</sup> required the estimation of the empirical C<sub>9</sub> unit formula of k-lignin in order to compare the NMR results with the OH number determined by titration following the ISO 14900:2001(E) standard. Therefore, the estimation of the empirical C<sub>9</sub> unit formula, which is shown in Table 2, was calculated according to the values obtained by elemental analysis and the methoxyl group (OCH<sub>3</sub>) content calculated by the integration of the signal at 56.6 ppm of the <sup>13</sup>C spectrum of k-lignin. The value of the integrations of methoxyl, carbonyl and carboxyl groups calculated in k-lignin (number of carbon atoms per C<sub>9</sub>unit) together with the values of corresponding to the OH(I), OH(II) and OH(ϕ) content calculated in the carbonyl region of ac-lignin, are shown in Table 4. The molecular weight value obtained per C<sub>9</sub> unit (Table 2) is in accordance with the values reported for other softwood kraft lignins, which are usually around 180 g mol<sup>-1</sup> (Crestini, 2012). The total hydroxyl content calculated by <sup>13</sup>C NMR (6.96 mmol g<sup>-1</sup>) approaches the value obtained by titration (7.33 mmol g<sup>-1</sup>). These values are similar to those reported by CA Cateto et al. (Cateto et al., 2008) for another commercial kraft lignin, although in their case the phenolic OH content was higher (3.95 mmol g<sup>-1</sup>). The aliphatic OH content in k-lignin is nearly twice times the amount of phenolic OH (often referred as the reactive group of lignin) (Paulsson and Simonson, 2002), being primary OH more abundant than secondary ones. The absence of signals corresponding to syringyl (S) units between 103 and 105 ppm (C-2, C-6 from S), and between 152 and 153 ppm (C-3 and C-5 from 4-O-alkylated S group) confirmed the predominant presence of guaiacyl (G) units, as it was expected owing to the softwood origin of k-lignin. These characteristic signals from carbons related to G units appear in the aromatic region of the <sup>13</sup>C NMR spectrum (Fig. 3), between 100 and 160 ppm.

The lignin functionalization with IPDI was confirmed qualitatively by <sup>13</sup>C-CP/MAS NMR spectroscopy (Fig. 4 and Table 5).

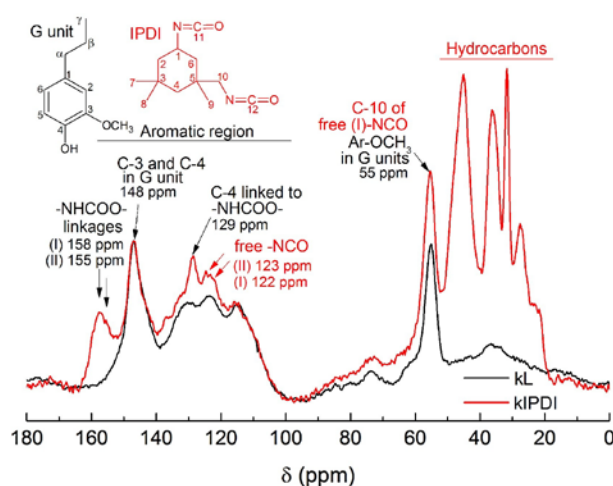


**Fig. 4.** <sup>13</sup>C-CP/MAS NMR spectra of k-lignin and k-IPDI.

**Table 5.**  $^{13}\text{C}$  CP/MAS NMR spectra signal assignments.

Sample	$\delta$ (ppm)	Assignment
k-IPDI	157.6	Secondary urethane linkage
	155.2	Primary urethane linkage
	146.9	Superposition C-3 and C-4 of G unit
	129.1	C-4 of G unit connected to -NHCOO-
	123.1	Free secondary -NCO
	122.4	Free primary -NCO
	56.6	Superposition aromatic -OCH <sub>3</sub> in G+primary carbon (C-10) of unreacted -NCO from IPDI
	45.1	Carbon attached to secondary isocyanate (C-1) from IPDI C-1 from unreacted secondary -NCO C-10 from reacted primary -NCO C-2 and C-4 (-CH <sub>2</sub> ) from IPDI C-1 and C-6 from reacted secondary -NCO
	36.2	-CH <sub>2</sub> - (C-6) from IPDI
	31.7	CH <sub>3</sub> - (C-7 and C-8) from IPDI
	27.6	CH <sub>3</sub> - (C-9) from reacted primary NCO
	23.1	CH <sub>3</sub> - (C-9) from unreacted primary NCO
	k-lignin	147.0
55.1		Aromatic methoxyl (-OCH <sub>3</sub> ) from G units

The appearance of new signals between 20 and 70 ppm corresponded to hydrocarbons of the isocyanate structure, whereas the reaction between the isocyanate and the hydroxyl groups from lignin was evidenced by the appearance of new signals corresponding to urethane (-NHCOO-) linkages at 155.2 and 157.6 ppm (secondary and primary urethane linkages, respectively). The new signal appearing at 129.1 ppm was attributed to C-4 from G unit connected to NHCOO-. The availability of free isocyanate groups for further reaction with the matrix was confirmed by the appearance of new signals at 122.4 and 123.1 ppm, corresponding to free primary and secondary NCO groups, respectively (Bialas et al., 1990), superimposed with the signals corresponding to aromatic carbons in lignin.

### 3.1.3. Morphology and particle size

As it can be observed in Fig. 5, k-IPDI is perfectly discernible from k-lignin, as the former presents

a yellowish color and a looser texture. SEM images (Fig. 5) revealed that k-IPDI presented a lower particle size than the unmodified k-lignin, probably due to changes in surface energy as a consequence of the modification with isocyanate, as it was suggested elsewhere (Chauhan et al., 2014). Nevertheless, the particle size of k-lignin was not relevant since it was added to the polyurethane formulation as a solution in THF, removing afterwards the solvent and keeping the k-lignin solved in the polyol. But in case of k-IPDI the particle size, ranging from 400 to 700 nm was significant as it was found to be insoluble in organic solvents and had to be added to the polyurethane formulation by direct mixing with the polyol

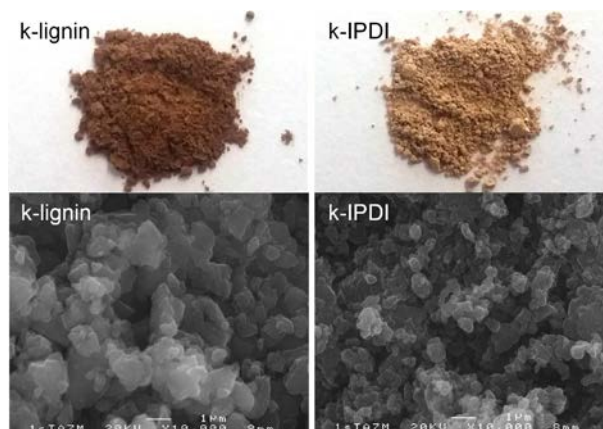


**Fig. 5.** Images and SEM micrographs of dried k-lignin (left) and k-IPDI (right). SEM micrographs with x10000 magnification.

#### 3.1.4. *Thermal properties*

The effect of isocyanate functionalization on the glass transition temperature ( $T_g$ ) of lignin was analyzed by DSC, removing previously the thermal history of the samples. Fig. 6 shows the DSC thermograms of k-lignin and k-IPDI. The  $T_g$  of k-lignin was found to be 151.2 °C, which was consistent with the reported values from other commercial kraft lignins (Gellerstedt, 2015; Lora, 2008). Nevertheless, it can be observed that the  $T_g$  in k-IPDI is shifted 112 °C below the  $T_g$  of the unmodified lignin, resulting in a  $T_g$  of 39.2 °C. This was attributed to the introduction of the urethane linkages that increased the mobility of the lignin structure as a consequence of the lower hydroxyl content, which resulted in the reduction of hydrogen bonding. Other works suggested that derivatization of lignin decreased the  $T_g$  value due to a plasticization effect of the derivatization process (Lisperguer et al., 2009).

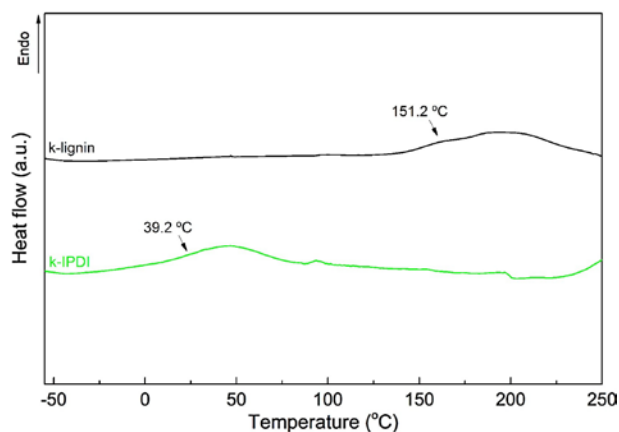


**Fig. 6.** DSC thermograms of k-lignin and k-IPDI.

Fig. 7 shows the thermal degradation of lignin under inert atmosphere, which was broader than that of the IPDI that presented a sharp mass loss at 221 °C. This was attributed to the different groups and heterogeneous molecular weight moieties forming the complex lignin structure. Fig. 7 and Table 6 show that the degradation of k-lignin occurred between 300 and 400 °C as a consequence of the cleavage of C-C and  $\beta$ - $\beta$  linkages of lignin's main structure (Ferryet al., 2015). The rearrangement of the lignin backbone occurred from 450 °C, giving place to high yields of char (39.87% in k-lignin). The maximum degradation temperature was shifted 50 °C towards lower temperatures in k-IPDI as a consequence of the combined degradation of the urethane linkages formed between the isocyanate and the lignin. Despite the previous drying of k-lignin and the organic modification of k-IPDI, some amount of volatile compounds and remaining moisture was lost between 65 and 105 °C (2 and 3%, respectively). The lack of residue in the degradation of IPDI contributed to decrease the residue of k-IPDI a 37% with respect to k-lignin. Hence, the functionalization of lignin produced a decrease on its thermal stability.

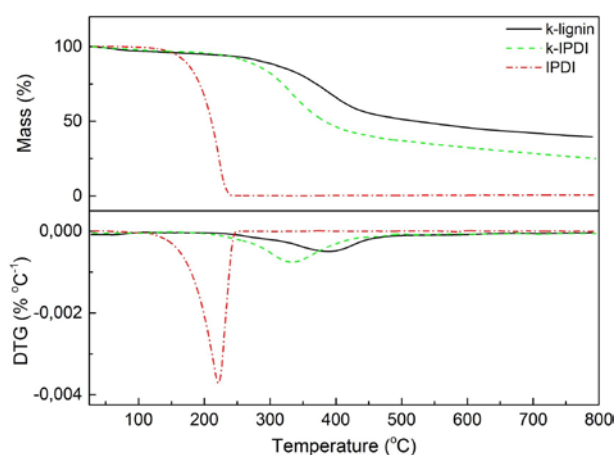


**Fig. 7.** Mass loss (up) and first derivative (down) curves of k-lignin and k-IPDI.

**Table 6.** Glass transition and degradation temperatures of k-lignin and k-IPDI obtained by DSC and TGA**Table 6. Glass transition and degradation temperatures of k-lignin and k-IPDI obtained by DSC and TGA.**

	<b>T<sub>g</sub> (°C)</b>	<b>T<sub>max</sub> (°C)</b>	<b>Mass loss<sub>1</sub> (wt%)</b>	<b>Residue at 800°C (wt%)</b>
k-lignin	151.2	386	60.15	39.87
k-IPDI	39.2	333	74.83	25.04

T<sub>max</sub>: Temperature at maximum degradation rate.

### 3.2. Characterization of polyurethane foams

#### 3.2.1. Effect of lignin in the polymerization process

The effect of the presence of k-lignin and k-IPDI in the reactivity of the polyurethane foam formation was studied by FTIR (Fig. 8), calculating the area of the remaining isocyanate stretching vibration at 2276 cm<sup>-1</sup> 24 h after the polymerization, and normalizing it with respect to the signal of a group that did not take part into the polymerization process, e.g. the C=C aromatic stretching vibration at 1598 cm<sup>-1</sup>. The area of this band was deconvoluted and calculated in PUF-REF and was taken as a reference, since the lignin contributed also with C=C groups. Table 7 shows NCO/C=C ratio and the timings of the different steps of the foaming process, as well as the maximum height of the final foams. It can be observed in Table 7 that the timings of the different foaming stages increased when both unmodified and IPDI-modified lignin were added to the foam, suggesting that its complex structure hindered the reaction between the hydroxyl groups of the polyol and the isocyanate, as it can also be appreciated in the increase of the NCO/C=C ratio.

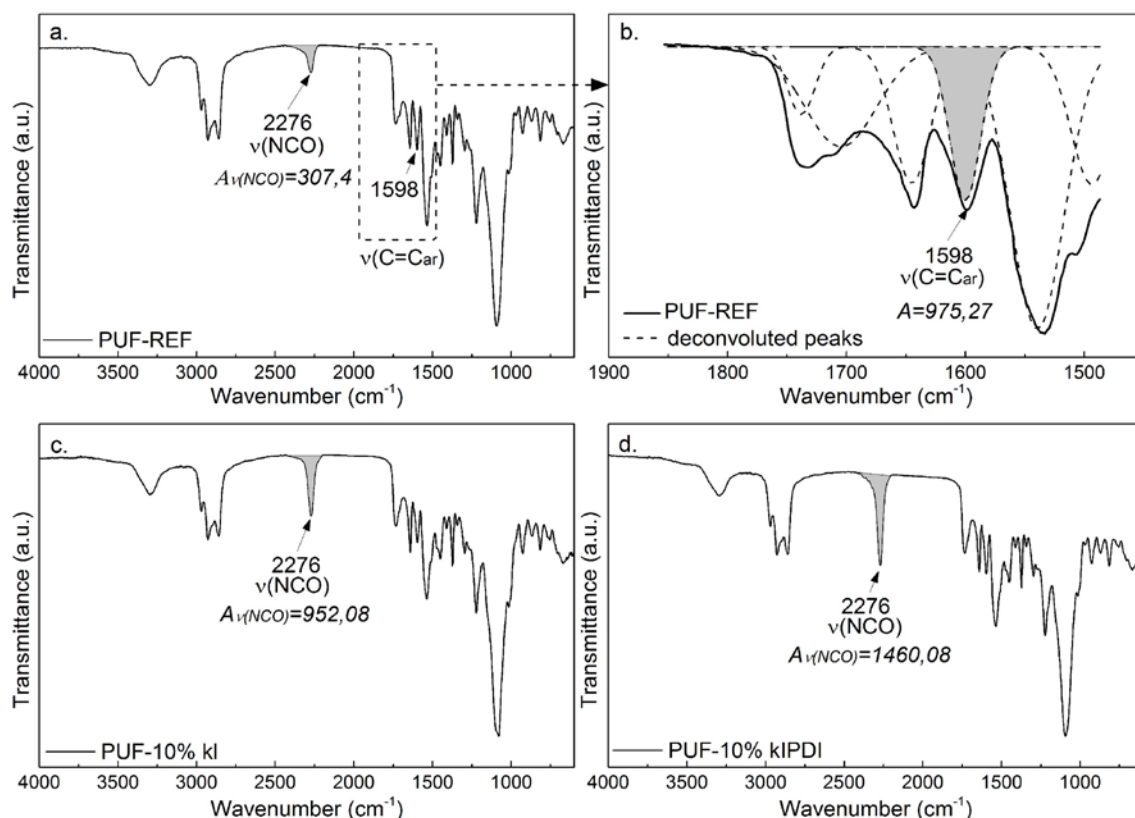


**Fig. 8.** FTIR spectra of PUF-REF(a), deconvolution of the aromatic C=C band in PUF-REF (b), PUF-10%kl (c) and PUF-10%kIPDI (d).

**Table 7.** Reaction times of the different stages in the foaming process and NCO/C=C ratio.

Sample	Cream time (s)	Rise time (s)	Gel time (s)	Tack-free time (h)	Max. height (mm)	Area $\nu(\text{NCO})/\text{C}=\text{C}$
PUF-REF	7	83	160	2.00	98	0.315
PUF-3%kl	11	88	167	3.00	88	0.709
PUF-5%kl	15	124	260	4.50	84	0.869
PUF-10%kl	23	225	859	6.00	73	0.976
PUF-3%kIPDI	20	125	300	3.83	95	0.969
PUF-5%kIPDI	24	163	310	4.25	87	0.973
PUF-10%kIPDI	26	168	632	5.83	75	1.497

Comparing the timings between k-lignin and k-IPDI containing foams, it is mandatory to take into consideration that the used catalyst quantity had to be increased in case of k-lignin containing foams to avoid the collapse of the structure, as a consequence of the decrease in polymerization rate caused by the presence of lignin. The effect of this higher catalyst content was clearly observed in the lower cream, rise and gel time values and lower NCO/C=C ratios at low k-lignin content, since this accelerating effect was lost at 10% k-lignin content. The use of

this catalyst formulation in k-IPDI containing foams caused their shrinkage due to the exceeding catalyst content, so it was expected that if it could be possible to prepare foams with the same catalyst formulation, the timings of the k-lignin containing ones would be much higher than those containing k-IPDI.

### 3.2.2. Density, cell size and lignin attachment to the foam

Density is a key parameter in the final properties of the materials, since the mechanical properties depend directly apart from the nature of the material, on the amount of the material available and its distribution along the cellular structure. Table 8 shows that despite all foams were prepared using the same blowing agent amount, meaning that the same amount of CO<sub>2</sub> was generated during the foaming process, the addition of either k-lignin or k-IPDI contributed to increase the density of the foams.

**Table 8.** Density, average cell size, strut width, open cell content, viscosity of the polyol-lignin mixture and mass loss after extraction of the k-lignin and k-IPDI containing foams.

**Table 8. Density, average cell size, strut width, open cell content, viscosity of the polyol-lignin mixture and mass loss after extraction of the k-lignin and k-IPDI containing foams.**

Sample	Density (kgm <sup>-3</sup> )	Average cell size (μm)	Average strut width (μm)	Open cell content (%)	Viscosity of the polyol-lignin mixture (mPas)	Mass loss after extraction (wt.%)
PUF-REF	32.4±0.8	215.7±58.3	39.7±7.5	21.7±0.6	837	–
PUF-3%kl	32.3±0.2	202.5±65.6	59.5±12.0	30.3±1.5	1265	0.48
PUF-5%kl	36.2±0.3	197.1±51.0	63.7±11.7	32.7±2.1	1458	3.31
PUF-10%kl	42.2±0.3	176.5±59.3	89.4±25.0	36.0±4.3	1837	3.85
PUF-3%kIPDI	34.5±0.9	220.1±59.3	55.9±8.7	49.2±2.5	1283	0.53
PUF-5%kIPDI	36.9±0.6	233.6±62.1	66.7±14.4	54.7±4.2	1743	1.02
PUF-10%kIPDI	41.8±0.7	204.2±53.2	88.0±18.3	55.7±1.5	3497	1.12

As it was mentioned before, the addition of lignin increased the gelling time that could lead to the loss of CO<sub>2</sub> during the polymerization, resulting in structures with smaller cells and thicker walls, yielding higher density values as it was reported elsewhere (Mahmood et al., 2015). The lower size of the cells and the higher width of the struts were attributed to the increase in the viscosity of the polyol-lignin mixture, being the values in accordance with the density values, as they contained more material in the same volume. It is noteworthy that in general the density and the average cell size and strut width values evolve in the same extent regardless of the type of used lignin, having slightly higher average cell size values in case of k-IPDI containing foams, probably due to its higher reactivity. Fig. 9 shows SEM images of foam sections perpendicular to the growth (Fig. 9a) and also in growth direction (Fig. 9b). It can be observed that the cellular structure of the reference foam is formed by both small and large voids with thin struts. Also, it

can be observed that the cells are slightly larger in the growth direction, denoting that the foam rise took place rapidly giving place to elongated cells. This oriented effect was hindered in foams containing lignin, where more homogeneous pores and wider struts were observed, which could be attributed to the higher viscosity of the part B reactant mixture.

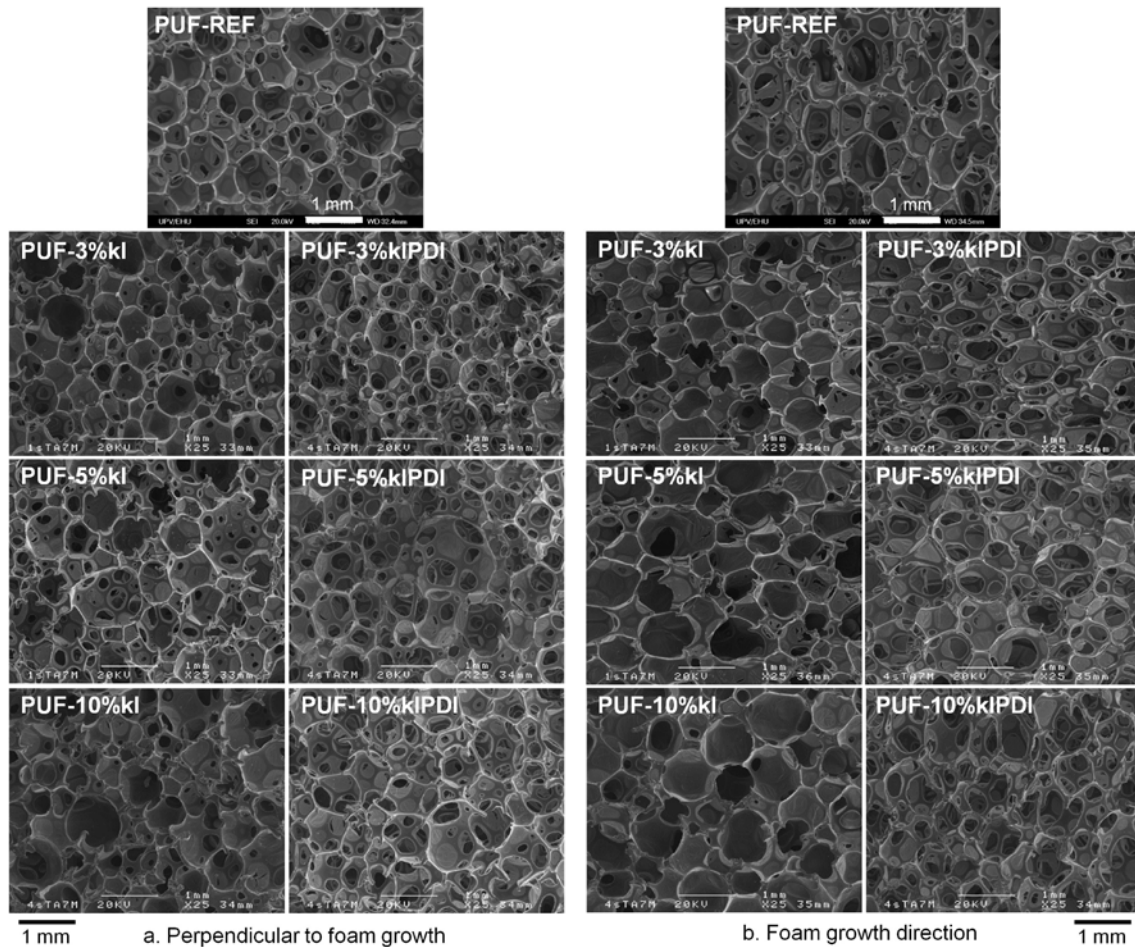


**Fig. 9.** SEM images of the sections perpendicular (a) and parallel (b) to foam growth, of PUF-REF and foams containing k-lignin and k-IPDI.

It shall be noted that the k-IPDI containing foams presented more voids in their walls suggesting the presence of more open cells. This higher open cell content was confirmed by measuring the air passing through the structure of the foam, as shown in Table 8. Both k-lignin and k-IPDI containing foams present higher open cell content than PUF-REF, since lignin particles act as a breaking point of the cell walls. Notwithstanding, k-IPDI containing foams show more open cells than unmodified lignin containing ones. This could be owing to the fact that k-lignin was introduced in the formulation in solution with THF, resulting in a more homogeneous distribution of the lignin in the matrix, while k-IPDI was introduced by dispersing the solid into the polyol. The presence of these coarser distributed solid particles could enhance in a higher extent the breakage of the walls.

The interaction between lignin and polyurethane matrix was determined extracting foams with a dioxane/water (9/1, v/v) mixture, which is a good medium for dissolving lignin. The PUF-REF mass loss after the extraction was registered in order to take into account only the lignin mass

loss in the k-lignin and k-IPDI containing foams as shown in Table 8. As it can be observed, in both k-lignin and k-IPDI, the extracted lignin content is lower than the added. This suggested that part of the k-lignin was also chemically linked to the polyurethane matrix, but in lesser extent than k-IPDI, as a consequence of the isocyanate groups anchored to k-IPDI. These results suggested that the presence of isocyanate groups in lignin increased its reactivity. The chemical linkage of the lignin would prevent it from migration during its application.

### 3.2.3. Thermal properties

The determination of the glass transition temperature was performed by DSC. Table 9 and Fig. 10 thermograms show the T<sub>g</sub> of the different polyurethane foams, which are in accordance with T<sub>g</sub> values reported before for flexible PUF (Herrington and Hock, 1998). It can be observed that the presence of k-lignin yielded to slightly higher T<sub>g</sub> values, in the same way as it was reported before (Wanget al., 2013; Yoshida et al., 1990). This effect was attributed to the fine dispersion of k-lignin in the polyurethane matrix as a consequence of its introduction in THF solution into the formulation. This finer dispersion, together with the higher T<sub>g</sub> of k-lignin, could cause the increase of the T<sub>g</sub> values of k-lignin containing foams as a result of the increased interaction between lignin and the matrix. In contrast, the rougher dispersion of k-IPDI through the matrix and its lower T<sub>g</sub> value, resulted in lower lignin-matrix interactions, which was reflected in a slight decrease in the T<sub>g</sub> of the k-IPDI containing foams.

**Table 9.** Glass transition and thermal degradation temperatures of the prepared polyurethane foams.

	T <sub>g</sub> (°C)	T <sub>initial</sub> (°C)	T <sub>max1</sub> (°C)	T <sub>max2</sub> (°C)	Residue at 800°C (wt.%)
PUF-REF	-53.0	266.7	296.6	396.6	0.00
PUF-3%kl	-52.6	269.1	298.6	392.5	1.97
PUF-5%kl	-51.6	269.9	299.5	395.3	3.73
PUF-10%kl	-50.8	262.2	294.8	396.1	5.52
PUF-3%kIPDI	-54.1	267.4	293.8	399.4	1.89
PUF-5%kIPDI	-54.2	268.6	296.9	400.8	3.23
PUF-10%kIPDI	-53.6	267.9	293.9	402.6	4.85

T<sub>g</sub>: Glass transition temperature measured by DSC as the midpoint of the slope change.

T<sub>initial</sub>: Temperature at 5% weight loss.

T<sub>max1</sub> and T<sub>max2</sub>: Maximum degradation rate temperature of first and second stages, respectively.

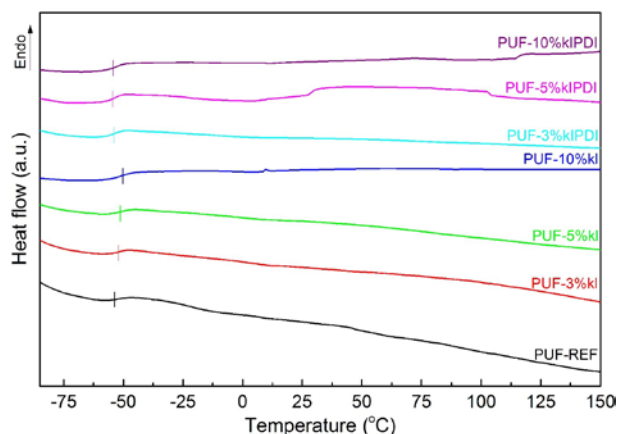


**Fig. 10.** DSC thermograms of the k-lignin and k-IPDI containing polyurethane foams.

The thermal stability of the flexible polyurethane samples was analyzed by TGA as shown in Fig. 11, and the most characteristic values are included in Table 9. It can be observed that the degradation took place in two stages regardless of the presence of both types of lignin. The first degradation step corresponded to the degradation of the isocyanate-related domains whereas the second step was attributed to the decomposition of the soft domains, which are related to the polyol.  $T_{initial}$  shifted slightly towards higher temperatures in case of PUF containing k-lignin, probably due to the stabilizing effect of the lignin particles distributed along the polyurethane matrix, whereas it remained practically unaltered in case of k-IPDI containing foams. In regard of the first stage maximum degradation temperature ( $T_{max1}$ ), it decreased in case of k-IPDI containing foams, as it was expected from the previous TGA analysis of k-IPDI, since it presented lower thermal stability than k-lignin, which contributed to delay between 2 and 3 °C the first degradation of PUF. Moreover, it should be noted that the weight loss related to this step decreased in both kinds of lignin containing foams, being function of the lignin content. Even though the presence of k-IPDI did not contribute to improve the thermal stability of the first stage of degradation, the chemical attachment of the lignin with the polymeric matrix contributed to increase up to 6 °C the maximum mass loss rate in the second stage. In relation to the residue, as it was expected, more quantity was formed with increasing lignin content; in higher extent in case of k-lignin (5.52% in case of PUF-10%kl) than k-IPDI (up to a 4.85% in case of PUF-10%kIPDI) owing to the low thermal stability of the urethane-urea linkages formed between the isocyanate modified lignin.

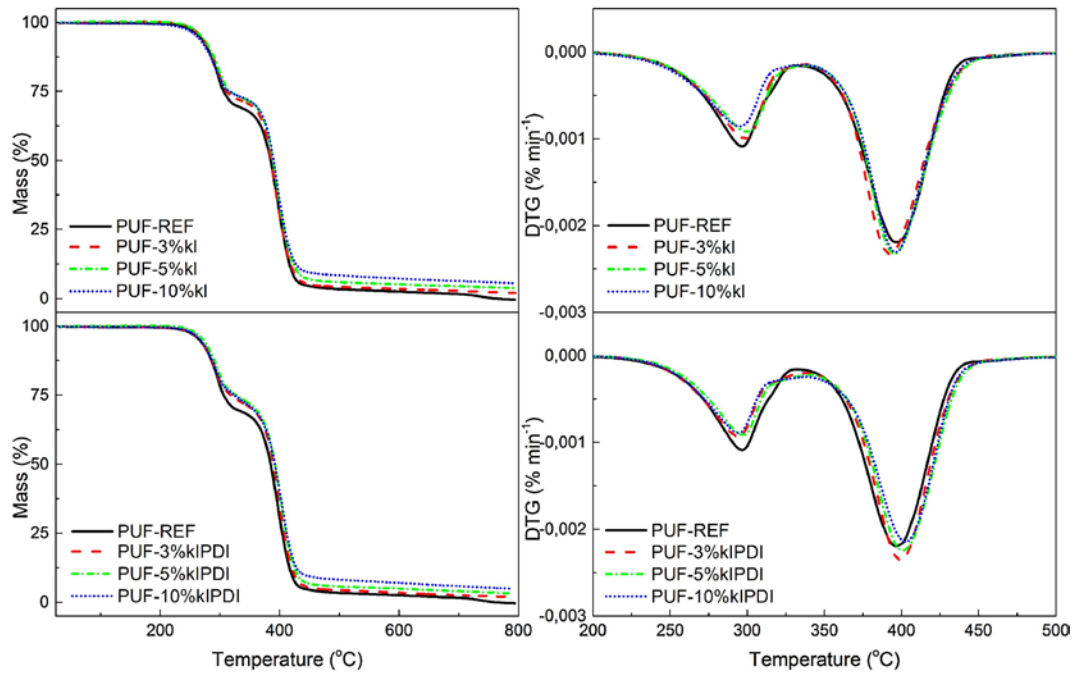


**Fig. 11.** TGA (left) and DTG (right) curves of the reference and k-lignin and k-IPDI containing foams.

#### 3.2.4. Mechanical properties

Resilience is a measure of the capacity of the foam to absorb elastic energy and to recover its original shape after being deformed. Therefore, resilience gives an insight into the support of the foam. The unique structure of foams, made of flexible struts, membranes and voids, allow them to support large deformations and recover their original shape with different recovery rates depending on the characteristics of the material (Avalle et al., 2001). The values showed on Table 10 demonstrated that the addition of k-lignin yield to less resilient, i.e. more viscoelastic foams, showing a delayed time to recover their original shape. Apart from other parameters, resilience could be related to the density of the foam, therefore those with lower density would take less time to recover (Millset al., 2009). This is fulfilled in case of k-lignin containing foams, which resilience decreases at higher density (and higher lignin content). In case of k-IPDI filled foams, the resilience decreases a 15% when adding a 3% k-IPDI and remains practically constant with increasing k-IPDI content, in spite of their higher density.

**Table 10.** Mechanical properties of the prepared flexible polyurethane foams: specific compressive stress given at 10% strain and energy absorption per volume unit until 50% strain.

	<b>Resilience (%)</b>	<b>CFD (kPa)</b>	<b>Specific compressive stress at 10% (<math>\text{kgm}^{-3})^{-1}</math>)</b>	<b>Specific modulus (kPa (<math>\text{kgm}^{-3})^{-1}</math>)</b>	<b>Energy absorption/volume at 50% (<math>\text{Jm}^{-3}\text{10}^{-2}</math>)</b>
PUF-REF	45.8±1.1	4.46±0.33	0.10	3.05	192.97
PUF-3%kl	40.0±0.8	6.06±0.33	0.11	2.36	200.71
PUF-5%kl	34.8±0.9	6.81±0.10	0.14	2.86	250.27
PUF-10%kl	33.3±0.3	9.51±0.15	0.13	3.17	312.23
PUF-3%kIPDI	39.1±0.3	4.59±0.41	0.11	2.29	172.09
PUF-5%kIPDI	38.9±0.8	5.21±0.13	0.06	1.82	120.74
PUF-10%kIPDI	38.7±0.3	5.53±0.29	0.03	1.58	103.33

On the other hand, the CFD value is a measure of the firmness of the foam, which is one of the most important characteristics of the flexible foams together with their density. Table 10 shows that the addition of lignin to the cellular polyurethane caused an increase in the CFD value of the foams. Unmodified lignin containing foams resulted to be more rigid than those containing k-IPDI due to the rougher particle dispersion

The compressive stress-strain curves (Fig. 12a) of the lignin containing foams show that those containing k-lignin presented a higher elastic modulus than PUF-REF, having the highest modulus at a k-lignin load of 10%. The opposite effect was observed in k-IPDI containing foams, presenting modulus below that of the PUF-REF, being especially low in case of 10% k-IPDI containing foam. Nevertheless, in order to avoid the effect of the density in the compressive characteristics of the foams, the specific compressive stress at 10% strain and the specific compressive modulus were calculated. The trend followed by the CFD values was confirmed with higher specific compressive stress values than PUF-REF in case of k-lignin containing foams. The specific modulus did not change much in case of k-lignin containing foams with respect to PUF-REF, but did present a growing trend at higher k-lignin content, whereas more flexible foams were obtained using k-IPDI presenting lower specific compressive stress at 10% strain and lower specific modulus than PUF-REF. Additionally, the energy absorption per unit volume of foam (toughness) was calculated as the area below the stress-strain curves until 50% deformation. This parameter is critical in applications involving safety, such as seat cushioning in automotive industry, where the foam act as a passive protective element for the dissipation of the energy absorbed during the impact.

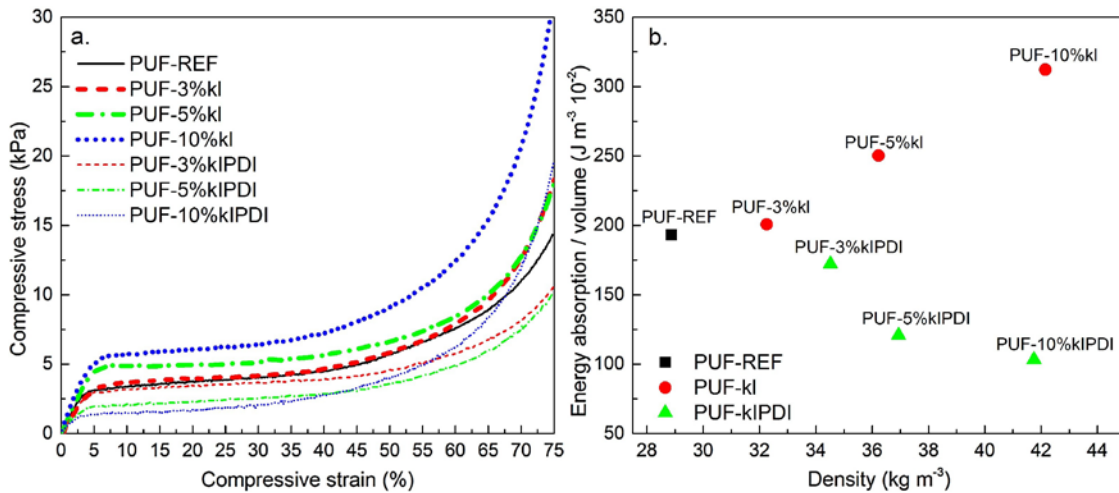


**Fig. 12.** Compressive stress-strain curves (a) and energy absorption capability according to density (b) of foams containing k-lignin and k-IPDI.

Fig. 12b shows the different trend followed by foams containing k-lignin and k-IPDI. The higher stiffness of k-lignin containing foams provides higher energy absorption capacity with higher lignin content, while k-IPDI containing samples present a lower area under the curve due to their higher flexibility, thus having a lower ability to absorb energy.

#### 4. Conclusions

A commercial softwood kraft lignin (k-lignin) was successfully functionalized with an aliphatic diisocyanate (IPDI) in order to increase its chemical attachment to a flexible polyurethane foam matrix. Approximately half of the hydroxyl groups present in lignin reacted with IPDI, as it was suggested by the OH consumption determined in k-IPDI by the ISO 14900:2001(E) standard, which was in agreement with the nitrogen content detected by elemental analysis. Its functionalization was also confirmed by FTIR and <sup>13</sup>C-CP/MAS NMR spectroscopy, through the appearance of new signals related to urethane groups and free isocyanate groups. Thermogravimetric analyses also showed that the degradation of k-IPDI occurred in one stage, having a maximum degradation temperature intermediate to that of k-lignin and neat IPDI. Moreover, flexible polyurethane foams containing 3, 5 and 10% lignin as an additive were successfully manufactured. It was observed that the presence of lignin hindered the foam formation increasing the times for each stage of the foaming process with higher lignin contents. This was more pronounced in case of k-lignin containing foams, that needed more catalyst amount in order to avoid the foam collapse due to the slower polymerization caused by the presence of lignin. Density increased in both k-lignin and k-IPDI containing foams, regardless the type of lignin, owing to the higher viscosity of the reactive mixture. More rigid foams were obtained with the addition of k-lignin to the polyurethane matrix, as it was observed by the higher CFD values obtained, suggesting that k-lignin acted as reinforcement in the polyurethane matrix. This reinforcing effect was also reflected in higher resilience values, meaning that k-lignin containing foams needed more time to recover their original shape. The lower resilience and CFD of k-IPDI containing foams was a consequence of the less fine dispersion compared to foams containing k-lignin. Regarding the strain-stress curves, it was observed that the modulus and the ability to absorb energy increased in k-lignin containing foams, whereas those

containing k-IPDI were more soft (with lower elastic modulus) but with lower energy absorption capacity. These properties will condition the application field of these foams. High energy absorption capacity would be needed in protective or safety-related applications, while comfort intended ones would be more focused on the flexibility of the foam.

## Acknowledgments

Financial support from the Basque Government in the frame of Grupos Consolidados (IT-776-13), from the Spanish Ministry of Economy and Competitiveness (MINECO) (MAT2013-43076-R) is gratefully acknowledged. Additionally, the author thanks the University of the Basque Country (UPV/EHU) for funding this work (PIF//13/079). Technical support provided by SGiker (UPV/EHU, MINECO, GV/EJ, ESF) is gratefully acknowledged.

## References

- Ashida, K., 2006. Polyurethane and Related Foams. Chemistry and Technology. CRC Press, Boca Ratón.
- Avalle, M., Belingardi, G., Montanini, R., 2001. Characterization of polymeric structural foams under compressive impact loading by means of energy-absorption diagram. *Int. J. Impact Eng.* 25, 455–472, [http://dx.doi.org/10.1016/S0734-743X\(00\)00060-9](http://dx.doi.org/10.1016/S0734-743X(00)00060-9).
- Barakat, A., Bagniewska-Zadworna, A., Frost, C.J., Carlson, J.E., 2010. Phylogeny and expression profiling of CAD and CAD-like genes in hybrid *Populus* (*P. deltoides* × *P. nigra*): evidence from herbivore damage for subfunctionalization and functional divergence. *BMC Plant Biol.* 10, 100, <http://dx.doi.org/10.1186/1471-2229-10-100>.
- Bialas, N., Höcker, H., Marschner, M., Ritter, W., 1990. <sup>13</sup>C NMR studies on the relative reactivity of isocyanate groups of isophorone diisocyanate isomers. *Macromol. Chem. Phys.* 185, 1843–1852, <http://dx.doi.org/10.1002/macp.1990.021910810>.
- Bouxin, F.P., McVeigh, A., Tran, F., Westwood, N.J., Jarvis, M.C., Jackson, S.D., 2015. Catalytic depolymerisation of isolated lignins to fine chemicals using a Pt/alumina catalyst: part 1—impact of the lignin structure. *Green Chem.* 17, 1235–1242, <http://dx.doi.org/10.1039/C4GC01678E>.
- Calvo-Correas, T., Santamaria-Echart, A., Saralegi, A., Martin, L., Valea, Á., Corcuera, M.A., Eceiza, A., 2015. Thermally-responsive biopolyurethanes from a biobased diisocyanate. *Eur. Polym. J.* 70, 173–185, <http://dx.doi.org/10.1016/j.eurpolymj.2015.07.022>.
- Cateto, C.A., Barreiro, M.F., Rodrigues, A.E., Brochier-Salon, M.C., Thielemans, W., Belgacem, M.N., 2008. Lignins as macromonomers for polyurethane synthesis: a comparative study on hydroxyl group determination. *J. Appl. Polym. Sci.* 109, 3008–3017, <http://dx.doi.org/10.1002/app.28393>.
- Cateto, C.A., Barreiro, M.F., Rodrigues, A.E., Belgacem, M.N., 2009. Optimization study of lignin oxypropylation in view of the preparation of polyurethane rigid foams. *Ind. Eng. Chem. Res.* 48, 2583–2589, <http://dx.doi.org/10.1021/ie801251r>.
- Chauhan, M., Gupta, M., Singh, B., Singh, A.K., Gupta, V.K., 2014. Effect of functionalized lignin on the properties of lignin-isocyanate prepolymer blends and composites. *Eur. Polym. J.* 52, 32–43, <http://dx.doi.org/10.1016/j.eurpolymj.2013.12.016>.
- Cinelli, P., Anguillesi, I., Lazzeri, A., 2013. Green synthesis of flexible polyurethane foams from liquefied lignin. *Eur. Polym. J.* 49, 1174–1184, <http://dx.doi.org/10.1016/j.eurpolymj.2013.04.005>.

Ciobanu, C., Ungureanu, M., Ignat, L., Ungureanu, D., Popa, V.I., 2004. Properties of lignin-polyurethane films prepared by casting method. *Ind. Crops Prod.* 20,231–241, <http://dx.doi.org/10.1016/j.indcrop.2004.04.024>.

Crestini, C., 2012. Conversion of lignin: chemical technologies and biotechnologies. In: Aresta, M., Dibenedetto, A., Dumeignil, F. (Eds.), *Biorefinery—From Biomass to Chemicals and Fuels*. Walter de Gruyter GmbH, Berlin/Boston, pp. 167–206, <http://dx.doi.org/10.1515/9783110260281.167>.

Dence, C.W., 1992. The determination of lignin. In: Lin, S.Y., Dence, C.W. (Eds.), *Methods in Lignin Chemistry*. Springer-Verlag, Berlin, pp. 33–61, [http://dx.doi.org/10.1007/978-3-642-74065-7\\_3](http://dx.doi.org/10.1007/978-3-642-74065-7_3).

Faix, O., Argyropoulos, D.S., Robert, D., Neirinck, V., 1994. Determination of hydroxyl groups in lignins. Evaluation of <sup>1</sup>H-, <sup>13</sup>C-, <sup>31</sup>P-NMR, FTIR and wet chemical methods. *Holzforschung* 48, 387–394, <http://dx.doi.org/10.1520/D0850-11.1>.

Fan, H.X., Li, H.P., Liu, Z.H., Yang, F., Li, G., 2015. Production of fine chemicals by integrated photocatalytic degradation of alkali lignin solution in corrugated plate reactor and cyclic extraction technology. *Ind. Crops Prod.* 74, 497–504, <http://dx.doi.org/10.1016/j.indcrop.2015.05.027>.

Ferry, L., Dorez, G., Taguet, A., Otazaghine, B., Lopez-Cuesta, J.M., 2015. Chemical modification of lignin by phosphorus molecules to improve the fire behavior of polybutylene succinate. *Polym. Degrad. Stab.* 113, 135–143, <http://dx.doi.org/10.1016/j.polymdegradstab.2014.12.015>

Gómez-Fernández, S., Ugarte, L., Peña-Rodríguez, C., Zubitur, M., Corcuera, M.Á., Eceiza, A., 2016. Flexible polyurethane foam nanocomposites with modified layered double hydroxides. *Appl. Clay Sci.* 123, 109–120, <http://dx.doi.org/10.1016/j.clay.2016.01.015>.

Gellerstedt, G., 1992. Gel permeation chromatography. In: Lin, S.Y., Dence, C.W. (Eds.), *Methods in Lignin*. Springer-Verlag, Berlin, pp. 487–497, [http://dx.doi.org/10.1007/978-3-642-74065-7\\_34](http://dx.doi.org/10.1007/978-3-642-74065-7_34).

Gellerstedt, G., 2015. Softwood kraft lignin: raw material for the future. *Ind. Crops Prod.* 77, 845–854, <http://dx.doi.org/10.1016/j.indcrop.2015.09.040>.

Gordobil, O., Egüés, I., Llano-Ponte, R., Labidi, J., 2014. Physicochemical properties of PLA lignin blends. *Polym. Degrad. Stab.* 108, 330–338, <http://dx.doi.org/10.1016/j.polymdegradstab.2014.01.002>.

Gosselink, R.J.A., Abächerli, A., Semke, H., Malherbe, R., Käuper, P., Nadif, A., VanDam, J.E.G., 2004a. Analytical protocols for characterisation of sulphur-free lignin. *Ind. Crops Prod.* 19, 271–281, <http://dx.doi.org/10.1016/j.indcrop.2003.10.008>.

Gosselink, R.J.A., Snijder, M.H.B., Kranenbarg, A., Keijsers, E.R.P., De Jong, E., Stigsson, L.L., 2004b. Characterisation and application of NovaFiber lignin. *Ind. Crops Prod.* 20, 191–203, <http://dx.doi.org/10.1016/j.indcrop.2004.04.021>.

Herrington, R., Hock, K., 1998. Flexible Polyurethane Foams. Dow Chemical Co., Midland, MI. Holladay, J.E., White, J.F., Bozell, J.J., Johnson, D., 2007. Top Value-Added Chemicals from Biomass Volume II—Results of Screening for Potential Candidates from Biorefinery Lignin. *Pacific Northwest Natl. Lab.* II, pp. 87, <http://dx.doi.org/10.2172/921839>.

Kadla, J.F., Kubo, S., Venditti, R.A., Gilbert, R.D., Compere, A.L., Griffith, W., 2002. Lignin-based carbon fibers for composite fiber applications. *Carbon* N. Y. 40, 2913–2920, [http://dx.doi.org/10.1016/S0008-6223\(02\)00248-8](http://dx.doi.org/10.1016/S0008-6223(02)00248-8).

Laurichesse, S., Avérous, L., 2014. Chemical modification of lignins: towards biobased polymers. *Prog. Polym. Sci.* 39, 1266–1290, <http://dx.doi.org/10.1016/j.progpolymsci.2013.11.004>.

Li, Y., Mlynár, J., Sarkanen, S., 1997. The first 85% kraft lignin-based thermoplastics. *J. Polym. Sci. B: Polym. Phys.* 35, 1899–1910, [http://dx.doi.org/10.1002/\(sici\)1099-0488\(19970915\)35:12<1899:aid-polb5>3.0.co;2-l](http://dx.doi.org/10.1002/(sici)1099-0488(19970915)35:12<1899:aid-polb5>3.0.co;2-l)

Li, C., Zhao, X., Wang, A., Huber, G.W., Zhang, T., 2015. Catalytic transformation of lignin for the production of chemicals and fuels. *Chem. Rev.* 115, 11559–11624, <http://dx.doi.org/10.1021/acs.chemrev.5b00155>.

Lisperguer, J., Perez, P., Urizar, S., 2009. Structure and thermal properties of lignins: characterization by infrared spectroscopy and differential scanning calorimetry. *J. Chil. Chem. Soc.* 54, 460–463, <http://dx.doi.org/10.4067/S0717-97072009000400030>.

Lora, J., 2008. Industrial commercial lignins: sources, properties and applications. In: Belgacem, M.N., Gandini, A. (Eds.), *Monomers, Polymers and Composites from Renewable Resources*. Elsevier Ltd., Amsterdam, pp. 225–241, <http://dx.doi.org/10.1016/B978-0-08-045316-3.00010-7> (Chapter 10).

Lundquist, K., 1992. Proton (1H) NMR spectroscopy. In: Lin, S.Y., Dence, C.W. (Eds.), *Methods in Lignin Chemistry*. Springer-Verlag, Berlin, pp. 242–249, [http://dx.doi.org/10.1007/978-3-642-74065-7\\_17](http://dx.doi.org/10.1007/978-3-642-74065-7_17).

Mahmood, N., Yuan, Z., Schmidt, J., Xu, C.C., 2015. Preparation of bio-based rigid polyurethane foam using hydrolytically depolymerized Kraft lignin via direct replacement or oxypropylation. *Eur. Polym. J.* 68, 1–9, <http://dx.doi.org/10.1016/j.eurpolymj.2015.04.030>.

Mainka, H., Täger, O., Körner, E., Hilfert, L., Busse, S., Edelmann, F.T., Herrmann, A.S., 2015. Lignin—an alternative precursor for sustainable and cost-effective automotive carbon fiber. *J. Mater. Res. Technol.* 4, 283–296, <http://dx.doi.org/10.1016/j.jmrt.2015.03.004>.

Mills, N.J., Stämpfli, R., Marone, F., Brühwiler, P.A., 2009. Finite element micromechanics model of impact compression of closed-cell polymer foams. *Int. J. Solids Struct.* 46, 677–697, <http://dx.doi.org/10.1016/j.ijsolstr.2008.09.012>.

Morandim-Giannetti, A.A., Agnelli, J.A.M., Lanc, as, B.Z., Magnabosco, R., Casarin, S.A., Bettini, S.H.P., 2012. Lignin as additive in polypropylene/coir composites :thermal, mechanical and morphological properties. *Carbohydr. Polym.* 87, 2563–2568, <http://dx.doi.org/10.1016/j.carbpol.2011.11.041>.

Ono, H.-K., Jones, F.N., Pappas, S.P., 1985. Relative reactivity of isocyanate groups of isophorone diisocyanate. Unexpected high reactivity of the secondary isocyanate group. *J. Polym. Sci. Polym. Lett. Ed.* 23, 509–515, <http://dx.doi.org/10.1002/pol.1985.130231003>.

Passoni, V., Scarica, C., Levi, M., Turri, S., Griffini, G., 2016. Fractionation of industrial softwood kraft lignin: solvent selection as a tool for tailored material properties. *ACS Sustain. Chem. Eng.* 4, 2232–2242, <http://dx.doi.org/10.1021/acssuschemeng.5b01722>.

Paulsson, M., Simonson, R., 2002. Acetylation of lignin and photostabilization of lignin-rich mechanical wood pulp and paper. In: Hu, T.Q. (Ed.), *Chemical Modification, Properties and Usage of Lignin*. Springer Science + Business Media, LLC, New York, pp. 227–245, [http://dx.doi.org/10.1007/978-1-4615-0643-0\\_12](http://dx.doi.org/10.1007/978-1-4615-0643-0_12).

Rozman, H.D., Tan, K.W., Kumar, R.N., Abubakar, A., 2001. Preliminary studies on the use of modified ALCELL lignin as a coupling agent in the biofiber composites. *J. Appl. Polym. Sci.* 81, 1333–1340, <http://dx.doi.org/10.1002/app.1558>.

Sarkanen, S., Teller, D.C., Stevens, C.R., McCarthy, J.L., 1984. Associative interactions between kraft lignin components. *Macromolecules* 17, 2588–2597, <http://dx.doi.org/10.1021/ma00142a022>.

Soares, B., Gama, N., Freire, C.S.R., Barros-Timmons, A., Brandão, I., Silva, R., Neto, C.P., Ferreira, A., 2015. Spent coffee grounds as a renewable source for copolyols production. *J. Chem. Technol. Biotechnol.* 90, 1480–1488, <http://dx.doi.org/10.1002/jctb.4457>.

Stuart, B.H., 2004. Organic molecules. In: *Infrared Spectroscopy: Fundamentals and Applications*. Wiley & Sons, Ltd.,

Chichester, UK, pp. 71–93, <http://dx.doi.org/10.1002/0470011149.ch4>.

Szycher, M., 2013. Flexible and semiflexible foams. In: Szycher's Handbook of Polyurethanes. CRC Press, Boca Ratón, pp. 181–255, <http://dx.doi.org/10.1201/b12343-8> (Chapter 7).

Tejado, A., Kortaberria, G., Peña, C., Labidi, J., Echeverria, J.M., Mondragon, I., 2008. Isocyanate curing of novolac-type ligno-phenol-formaldehyde resins. *Ind. Crops Prod.* 27, 208–213, <http://dx.doi.org/10.1016/j.indcrop.2007.07.009>.

Wang, Z., Yang, X., Zhou, Y., Liu, C., 2013. Mechanical and thermal properties of polyurethane films from peroxy-acid wheat straw lignin. *BioResources* 8, 3833–3843.

Yoshida, H., Mörck, R., Kringstad, K.P., Hatakeyama, H., 1990. Kraft lignin in polyurethanes. II. Effects of the molecular weight of kraft lignin on the properties of polyurethanes from a kraft lignin polyether triol polymeric MDI system. *J. Appl. Polym. Sci.* 40, 1819–1832, <http://dx.doi.org/10.1002/app.1990.070401102>.

Zhang, W., Ma, Y., Wang, C., Li, S., Zhang, M., Chu, F., 2013. Preparation and properties of lignin-phenol-formaldehyde resins based on different biorefinery residues of agricultural biomass. *Ind. Crops Prod.* 43, 326–333, <http://dx.doi.org/10.1016/j.indcrop.2012.07.037>.